Task-Sensitive Reconfiguration of Corticocortical 6–20 Hz Oscillatory Coherence in Naturalistic Human Performance

Timo Saarinen,[1,2]* Antti Jalava,[1,2] Jan Kujala,[1] Claire Stevenson,[1] and Riitta Salmelin[1,2]

[1]*Brain Research Unit, O.V. Lounasmaa Laboratory, Aalto University, AALTO, Finland*
[2]*Aalto NeuroImaging, Aalto University, AALTO, Finland*

Abstract: Electrophysiological oscillatory coherence between brain regions has been proposed to facilitate functional long-range connectivity within neurocognitive networks. This notion is supported by intracortical recordings of coherence in singled-out corticocortical connections in the primate cortex. However, the manner in which this operational principle manifests in the task-sensitive connectivity that supports human naturalistic performance remains undercharacterized. Here, we demonstrate task-sensitive reconfiguration of global patterns of coherent connectivity in association with a set of easier and more demanding naturalistic tasks, ranging from picture comparison to speech comprehension and object manipulation. Based on whole-cortex neuromagnetic recording in healthy behaving individuals, the task-sensitive component of long-range corticocortical coherence was mapped at spectrally narrow-band oscillatory frequencies between 6 and 20 Hz (theta to alpha and low-beta bands). This data-driven cortical mapping unveiled markedly distinct and topologically task-relevant spatiospectral connectivity patterns for the different tasks. The results demonstrate semistable oscillatory states relevant for neurocognitive processing. The present findings decisively link human behavior to corticocortical coherence at oscillatory frequencies that are widely thought to convey long-range, feedback-type neural interaction in cortical functional networks. *Hum Brain Mapp 36:2455–2469, 2015.* © 2015 The Authors Human Brain Mapping Published by Wiley Periodicals, Inc.

Key words: task performance; behavior; cognition; functional neuroimaging; cerebral cortex; electrophysiology; connectome; functional brain network

INTRODUCTION

Neurocognition has been thought to rely on electrophysiological interactions and information transfer within large-scale functional brain networks [Friston, 2008; Mesulam, 2008; Siegel et al., 2012; Varela et al., 2001]. Oscillatory activity is a prominent feature of neuronal signaling [Buzsáki and Draguhn, 2004], and coherent oscillations between brain regions have been implicated in formation of functional connections and network structures [Bressler and Kelso, 2001; Fries, 2005; Siegel et al., 2012]. Coherence

Timo Saarinen and Antti Jalava contributed equally to this work

Contract grant sponsors: Academy of Finland (National Centres of Excellence Programme 2006–2011; personal grants to J.K. and R.S.); Sigrid Juselius Foundation; and Finnish Funding Agency for Technology and Innovation (SalWe Strategic Center for Science, Technology and Innovation in Health and Well-being)

*Correspondence to: Timo Saarinen; Brain Research Unit, O.V. Lounasmaa Laboratory, Aalto University, P.O. Box 15100, FI-00076 AALTO, Finland. E-mail: timo.p.saarinen@aalto.fi

Received for publication 2 July 2014; Revised 24 February 2015; Accepted 24 February 2015.

DOI: 10.1002/hbm.22784

Published online 11 March 2015 in Wiley Online Library (wileyonlinelibrary.com).

describes the mutual dependency of oscillatory components at the operational millisecond timescale of neural activity. Empirically, coherence has been demonstrated in dynamic episodes of interregional neuronal communication [Bosman et al., 2012; Bressler et al., 1993; Buschman and Miller, 2007; Pesaran et al., 2008; Salazar et al., 2012], and it is thought to promote functional coupling through periodically occurring electrical potentiation of signaling and temporal coordination of synchronous activity [Bressler and Kelso, 2001; Fries, 2005; Izhikevich, 2001; Siegel et al., 2012].

The primate cerebral cortex has been shown to utilize interregional coherence to support behavior [Bosman et al., 2012; Bressler et al., 1993; Buschman and Miller, 2007; Pesaran et al., 2008; Salazar et al., 2012]. Intracortical recordings in monkeys have found task-sensitive coherent activity between selected pairs of functionally relevant and anatomically connected but distant cortical sites [Buschman and Miller, 2007; Pesaran et al., 2008; Salazar et al., 2012]. Such long-range coherence can operate at several frequencies, including the prominently oscillatory range across the theta, alpha and beta bands (approximately 4–30 Hz) [Bastos et al., 2015; Bosman et al., 2012; Bressler et al., 1993; Buschman and Miller, 2007; Pesaran et al., 2008; Salazar et al., 2012; von Stein and Sarnthein, 2000]. Long-range coherence has also been demonstrated to link subpopulations of cortical neurons that contain information relevant for the task at hand [Bosman et al., 2012; Buschman and Miller, 2007; Pesaran et al., 2008; Salazar et al., 2012]. Coherence may thus facilitate task-sensitive routing of functional connections and inclusion of relevant information processing in the large-scale corticocortical network.

The present, noninvasive magnetoencephalography (MEG) coherence imaging study on human naturalistic performance builds up on these intracortical descriptions of coherent connections. Here, in a data-driven search across the cortex, we sought to characterize task-sensitive reconfiguration of the global patterns of coherent oscillatory connectivity. We studied performance within a set of naturalistic and low-constrained tasks [cf. Felsen and Dan 2005; Hasson et al. 2010; Ingram and Wolpert, 2011; Pesaran et al., 2008] that represent hallmarks of human behavior, including active vision, language ability and object manipulation. We applied a neuromagnetic imaging approach [Gross et al., 2001; Kujala et al., 2008] that allows direct sensor-to-cortex mapping of MEG coherence data into long-range corticocortical estimates, without resorting to any *a priori* seed regions, external reference signals or intermediate signal projections to the brain space [for a review on MEG connectivity, see Palva and Palva, 2012]. The present method of tracking coherent activity at the operational neural frequencies provides a whole-cortex imaging analog to the intracranial animal and patient coherence recordings that typically have more limited coverage [e.g., Buschman and Miller, 2007; Pesaran et al., 2008; Salazar et al., 2012; Sehatpour et al., 2008; Swann et al., 2012].

Task-sensitive coherence was determined for both easier (E) and more demanding (D) variants of visual picture comparison (easy distinct, more demanding nondistinct differences), speech comprehension (easy native, more demanding non-native language) and bimanual object manipulation (easy handling, more demanding solving of a Rubik's cube) tasks. These tasks were performed in a freely unfolding, subject-driven manner and they were designed to elicit distributed neurocognitive information processing that would tax differentially the perceptual, motor, attentional-executive, and memory abilities. The central goal was to determine whether the global connectivity patterns within each of the three behavioral modalities would show specific topology compared to a generic task-non-specific pattern. Building on the concept that elevated coherence indicates efficient interregional coupling and relevant connections for a task [Fries, 2005; Siegel et al., 2012], we focused on functional connections that would be more engaged in a particular task, rather than suppressed, compared to the task-non-specific baseline [cf. "task-positive" pattern; Fox et al., 2005]. Task-sensitivity was determined as increase of interregional coherence with respect to the mean pattern (task-mean) calculated across all the tasks. Importantly, the resulting connectivity estimates represent the modulated components of the coherent connectivity among the tasks and not a contrast to, for example, less well defined rest data [Morcom and Fletcher, 2007].

Task-related functional networks are a current and important theme in neuroscience [see Park and Friston, 2013]. By taking a step from the spontaneous rest activity and restricted, single-domain experimental protocols, we aimed for a data-driven view on task-sensitivity of functional oscillatory connectivity for a set of naturalistic human behaviors. In general, a proof-of-concept for functional large-scale networks as the basis of neurocognition is to uncover flexible functional connectivity patterns that feature both task-sensitivity and topological task-relevance. To achieve this, we quantified functional corticocortical connections using direct mapping of electrophysiological coherence at spectrally narrow-band, oscillatory frequencies. We hypothesized that neural oscillatory coherence would provide a key mechanism for the task-related network function. We further hypothesized that to fulfill the different neurocognitive requirements of each naturalistic task, the spatiospectral connectivity pattern, mediated by coherence, would show distinct task-specific modulation [task-sensitivity; see Engel et al., 2013; Siegel et al., 2012]. The topological pattern should not be sporadic but the cortical regions involved should cover task-associated regions (task-relevance) while overlapping in multidomain areas, such as frontoparietal cortex [Barbey et al., 2012; Duncan, 2010; Fox et al., 2005]. This study was conducted with an explorative approach to highlight the most prominent components of oscillatory connectivity that support

naturalistic performance. We successfully uncovered task-sensitive 6–20 Hz coherent connectivity patterns for each naturalistic task.

MATERIALS AND METHODS

Participants and Tasks

The participants were 10 right-handed, Finnish-speaking healthy adults (5 females; 5 males mean age 32 years, range 21–40 years). They gave their informed consent for the experiment, in agreement with a prior approval of the local Ethics Committee (Hospital District of Helsinki and Uusimaa; in compliance with Declaration of Helsinki). The subjects performed naturalistic tasks in three different modalities: visual, auditory, and sensorimotor. In each modality, task design was implemented as both an easy and a more demanding variant. Continuous task performance was monitored with video feed from the measurement room and questions (during pauses, see below) but no further quantification was made. The subjects were actively engaged with the tasks.

In the naturalistic visual tasks, the participants compared two color pictures of vegetation with differences in either highly distinct features (color modification in simplified photograph-based images with fine details removed; easier variant) or more subtle features (fine structural details present or not in photographs; more demanding variant). Comparison of these perceptually meaningful images required visual search and varying levels of visual attention and working memory. The stimuli were presented on a projector screen ~1 m away from the subject's eyes. The two pictures (width × height, ~12 × 8.5° per picture) were presented simultaneously, one above the other, for 30 s (altogether six picture pairs, 3 min of data in total). During a 7-s pause between stimulus presentations, the subjects were asked to indicate how many differences they found between the pictures, with the response given as finger lifts.

The naturalistic auditory conditions were speech comprehension tasks with sound track clips from fairly unknown Finnish-speaking movies (easier variant) and English-speaking movies (more demanding variant). The stimuli were delivered binaurally through nonmagnetic earplugs, at comfortable listening level. These speech comprehension tasks required concentration on verbal material embedded in natural environmental sounds and with a varying degree of linguistic challenge. All the Finnish-speaking subjects had studied English as part of their basic education (~10 years). There were three ~1-min clips, each followed by a 10-s pause during which the participants answered a question in Finnish about the content.

The naturalistic sensorimotor tasks were bimanual free manipulation of a Rubik's cube (without twisting it) and solving the Rubik's cube task, respectively, for 3 min. The Rubik's cube was a small (3 × 3 cm) nonmagnetic version, with the original 3-by-3 grid. Both tasks required visuomotor processing in object manipulation, and solving the Rubik's cube additionally demanded effortful visuospatial reasoning to guide the movements. None of the participants reported to be an expert in solving the Rubik's cube; to maintain the difficulty at a reasonable level, they were instructed to first try to align the color of only one side of the cube.

MEG Recordings and Procedure

MEG signals were recorded in a magnetically shielded room at the MEG Core, Aalto University, using a whole-head 306-channel system (102 triple sensor elements composed of two orthogonal planar gradiometers and one magnetometer; Elekta Oy, Helsinki, Finland). MEG data were passband filtered at 0.1–200 Hz and sampled at 600 Hz. The MEG recording was linked to the head anatomy with the help of four head position indicator coils that were attached to the participants's scalp: The locations of the coils with respect to three anatomical landmarks (nasion and preauricular points) were determined using a 3-D digitizer (Isotrak; Polhemus, Colchester, VT), and with respect to the MEG array by briefly energizing the coils before each recording session. Identification of the three anatomical landmarks on structural magnetic resonance images (MRIs) further allowed coregistration of MEG signals and the individual brain anatomy. The MRIs were acquired at the Advanced Magnetic Imaging Center, Aalto University, with a 3T Signa EXCITE MRI scanner (GE Healthcare). For behavioral monitoring, electro-oculography and the left and right arm electromyography were collected simultaneously with MEG.

The subjects were first introduced to the study and prepared for the measurement. Thereafter, they were seated under the MEG helmet and the different tasks were performed in separate blocks. These blocks were grouped by modality (visual, auditory, sensorimotor). The order of the three modalities, and of the tasks within each modality, was pseudorandomized across subjects.

MEG Data Processing and Connectivity Analysis

Preprocessing of the MEG data included application of the Spatiotemporal Signal Space Separation method (tSSS) to suppress noncerebral, artifactual signals (external noise, movement-related signals) [Taulu and Hari, 2009; Taulu and Simola, 2006]. This approach of separating and removing signals that do not originate in the brain/head space is based on physical properties of the MEG measure, that is, sensor geometry and electrodynamics, as well as statistical separation in the time domain.

For the characterization of corticocortical connectivity, we focused on frequencies that displayed the strongest coherence. This was estimated from the long-range (>10 cm) sensor–sensor coherence spectra, averaged across sensors for each task (Fig. 1). The frequencies below 20 Hz showed the

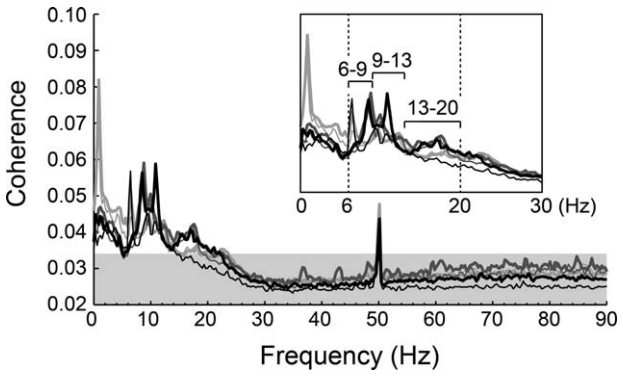

Figure 1.

Coherence as a function of frequency. Sensor–sensor coherence spectra, averaged across all sensors, with all task conditions overlaid (light gray lines, picture comparison; medium gray lines, speech comprehension; black lines, object manipulation; thicker lines for the easy and thinner lines for the demanding variants of the tasks). The top 20 % of the maximum coherence, across tasks and subjects, is reached in the area above the gray bar. Remnants of the power line 50-Hz artifact stand out as a narrow coherence peak. Inset: The subbands of the 6–20 Hz frequency range of interest are indicated (6–9 Hz, theta/low-alpha band; 9–13 Hz, high-alpha band; 13–20 Hz, low-beta band).

strongest coherence, across all tasks and subjects (cutoff at the highest 20%; see gray bar in Fig. 1). Naturalistic performance unavoidably enhances artifact signals. Therefore, to supplement tSSS preprocessing especially regarding eye and face muscle movements that are often difficult to fully remove from the brain-signal space and to secure cleanest possible data for the source-level connectivity estimation, the lowest frequencies (<6 Hz) were excluded from the analysis (note salient eye-movement related peak at ~1 Hz in the visual tasks in Fig. 1) [cf. Woestenburg et al., 1983]. As the broadband high frequency (gamma) activity showed overall much weaker coherence and is, furthermore, potentially contaminated by ocular and other muscle artifacts [Hipp and Siegel, 2013], it was excluded from the source-level analysis. Accordingly, we estimated corticocortical connectivity for the oscillatory (narrow-band) coherence in the 6–20 Hz frequency range.

Within the 6–20 Hz range, there were several spectral maxima (Fig. 1). The range was subdivided into three frequency bands of interest (inset in Fig. 1), corresponding to the commonly identified neural oscillatory bands (theta/low alpha, 6–9 Hz; high-alpha, 9–13 Hz; low-beta. 13–20 Hz) [cf. Bastos et al., 2015; Buzsáki and Draguhn, 2004; Cannon et al., 2014; von Stein and Sarnthein, 2000]. In this division, we chose to avoid exceedingly narrow bandwidths (<3 Hz). Two prominent spectral peaks (theta, low-alpha) fell within the 6–9 Hz band and one prominent peak (high-alpha) within the 9–13 Hz band. A somewhat less distinctive spectral component was observed in the 13–20 Hz band, featuring two maxima around 16 Hz.

A frequency-domain spatial filter approach, Dynamic Imaging of Coherent Sources (DICS) [Gross et al., 2001; Kujala et al., 2008], was applied to the MEG sensor-level data to obtain a brain-level estimate of long-range corticocortical coherence as a function of neural oscillatory frequencies. This source reconstruction method has two interesting properties. First, it performs a direct corticocortical mapping of sensor-level coherent activity, thus requiring no precursory signal projection to the brain-space and subsequent separate pair-wise connectivity analysis of the resulting source-level time courses. Second, it is based on temporally resolved signal cross-correlation, that is, linear dependence of oscillatory components in two time series as they evolve [Gross et al., 2001; Kujala et al., 2008; cf. Hipp et al., 2012]. Like any other M/EEG source reconstruction [Palva and Palva, 2012], the DICS estimate is nonunique and faces the problem of signal field spread which prevents reliable quantification of local (short-range) connectivity [Schoffelen and Gross, 2009]. The spatially smooth record of cortical activity provided by MEG is thus better suited for long-range connectivity analysis. DICS spatial filter can readily distinguish local maxima that are at least 2 cm apart [Liljeström et al., 2005]. We sought to suppress spurious connectivity [Schoffelen and Gross, 2009] by requiring a minimum distance of 4 cm between the connection start and end points and by focusing on contrasts between experimental conditions rather than absolute coherence values.

In the DICS analysis, first, a common grid of 9-mm side length, determined in one example brain, was transformed to cover cortical surface of the individual MRIs at corresponding grid sites (MNE Suite software; Hämäläinen, Martinos Center for Biomedical Imaging, Massachusetts. General Hospital, MA). To ensure best possible signal-to-noise ratio for the DICS estimation, we retained for further analysis 3,600 cortical grid points whose activity could be reliably picked up by the MEG helmet (i.e., grid points closest to the MEG sensors). The included grid points provided a good coverage of the cortical sheet (fissural and gyral). Second, cross-spectral density matrices across all planar-gradiometer sensor signals were computed for each task condition using Welch's averaged periodogram method (Hanning 2048-point window; 0.3 Hz resolution; 75% window overlap). These matrices contained information of linear oscillatory dependencies in the sensor-level data. Third, in a global all-to-all search, long-range coherence estimates (4 cm minimum distance) were computed for each cortical grid point with the other grid points in the frequency bands of interest using a DICS spatial filter.

To extract possible task-sensitive components of corticocortical connectivity, per frequency band, the global search results for each task were contrasted against the mean pattern calculated across all the tasks (task > task-mean). In addition, we tested pairwise comparisons between the easy and demanding variants of the tasks (E > D and D > E) within each task modality. To preclude changes of signal strength as an explanatory factor in the coherence-

based connectivity estimates [Schoffelen and Gross, 2009], we verified that the signal power was not significantly modulated by the task (task vs. task-mean; E vs. D) at any MEG sensor in a given contrast [$n = 10$; paired t-statistics, $P > 0.05$, false discovery rate (FDR) corrected]. If modulation was found, the frequency band in question was excluded from the further analysis of this particular task contrast.

Statistical significance of the coherent connections ($n = 10$; paired t-statistics, $P < 0.05$, FDR corrected) was determined on parcellated cortex (Fig. 2). The clustering of the grid points into <100 regions reduces the spatial sampling of the source-level data to a resolution that facilitates relative independence of the measurements. The regions of interest were generated in the common subject space, based on the Desikan-Killiany parcellation scheme [Desikan et al., 2006]. The Desikan-Killiany regions within 8.25 cm from the closest MEG sensor (Euclidean distance, average of grid points included in the region) and containing at least 10 grid points were retained in the analysis, resulting in a total of 75 regions (37 left; 38 right; Fig. 2). Mean coherence values for each of the regions were computed from the grid-based data per each subject, task and frequency band. Coherent connections between regions with a Euclidean distance of 1 cm or less between any of their vertex points were discarded; in practice, this meant that connections to border adjacent regions were excluded from the analysis. As a result, 418 connections were evaluated within the left hemisphere, 447 connections within the right hemisphere and 2221 connections when the whole cortex was considered at once. Significant coherence modulations were visualized on circular connectograms using a hierarchical bundling approach [Holten, 2006]. The statistical testing was conducted both within each hemisphere and also in the whole cortex, allowing interhemispheric connections.

Independence between the factors frequency band and task modality, as well as between frequency band and cortical area (frontal, central, cingulate, temporal, parietal, occipital), were tested with χ^2-statistics, using adjusted standardized residuals as *post hoc* indicators of which bands in which task modality or cortical area differed from the expected pattern (if independence between the factors does not hold). χ^2-statistics was also used to evaluate whether the observed distribution of significant coherent connections (pooled across the frequency bands) displayed a specific structure that differed from an equal distribution of connections (null hypothesis) per naturalistic task. For the χ^2-test the missing values due to the

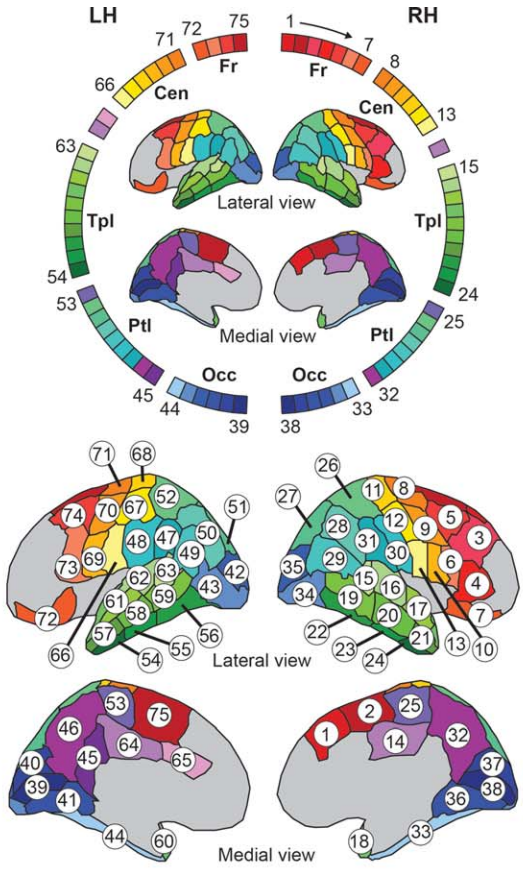

1	Sup. frontal gyrus (a)
2, 75	Sup. frontal gyrus (b)
3	Mid. frontal gyrus (a)
4	Inf. frontal gyrus (a)
5, 74	Mid. frontal gyrus (b)
6, 73	Inf. frontal gyrus (b)
7, 72	Orb. frontal cortex
8, 71	Precentral gyrus (a)
9, 70	Precentral gyrus (b)
10, 69	Precentral gyrus (c)
11, 68	Postcentral gyrus (a)
12, 67	Postcentral gyrus (b)
13, 66	Postcentral gyrus (c)
65	Ant. cingulate
14, 64	Post. cingulate
15, 63	Bank sup. temp. sulcus
16, 62	Sup. temporal gyrus (a)
17, 61	Sup. temporal gyrus (b)
18, 60	Sup. temporal gyrus (c)
19, 59	Mid. temporal gyrus (a)
20, 58	Mid. temporal gyrus (b)
21, 57	Mid. temporal gyrus (c)
22, 56	Inf. temporal gyrus (a)
23, 55	Inf. temporal gyrus (b)
24, 54	Inf. temporal gyrus (c)
25, 53	Paracentral lobule
26, 52	Sup. parietal cortex (a)
27, 51	Sup. parietal cortex (b)
28, 50	Inf. parietal cortex (a)
29, 49	Inf. parietal cortex (b)
30, 48	Supramarginal gyrus (a)
31, 47	Supramarginal gyrus (b)
32, 46	Precuneus
45	Isthmus cingulate
33, 44	Fusiform gyrus
34, 43	Lat. occipital cortex (a)
35, 42	Lat. occipital cortex (b)
36, 41	Lingual gyrus
37, 40	Cuneus
38, 39	Pericalcarine cortex

Figure 2.

Cortical parcellation scheme. Color codes for each cortical region (75 regions based on a Desikan-Killikany scheme [Desikan et al., 2006]) displayed on the surface views (lateral and medial) and on a circular connectogram. Numbering in the circular plot (running clock-wise; 1–38 right, 39–75 left hemisphere) corresponds to the regions indicated on the surface views. Region titles are listed below the figure. Note that there were a small number of regions that passed the criterion for selection in one hemisphere only: for 3 regions in the left and 2 regions in the right hemisphere, the homologous area in the other hemisphere was not included in the analysis. Abbreviations: LH, left hemisphere; RH, right hemisphere; Fr, frontal; Cen, central; Tpl, temporal; Ptl, parietal; Occ, occipital.

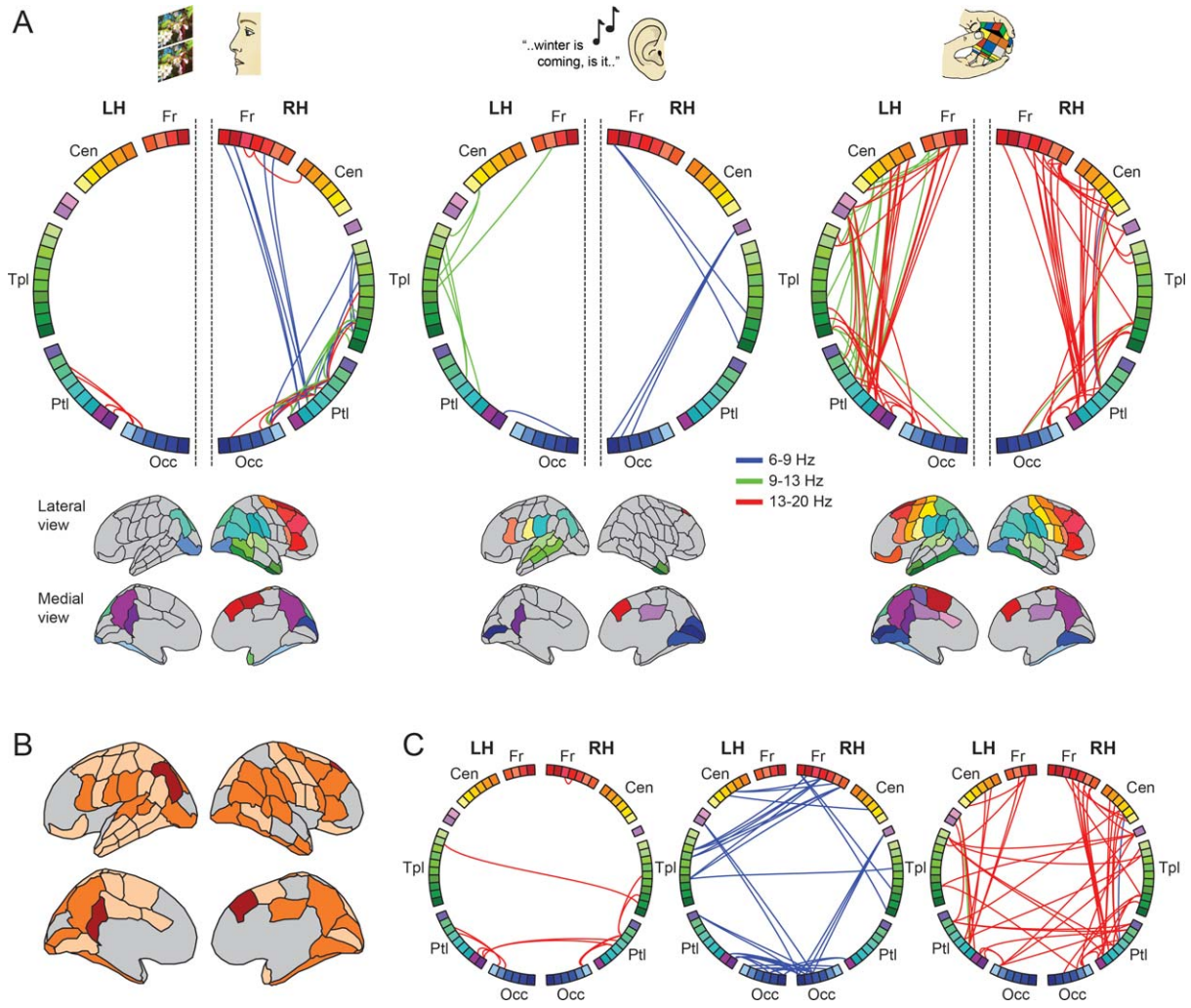

Figure 3.

Circular connectograms of significant task-sensitive coherent connectivity. (**A**) Within-hemisphere analysis for the three different modalities of naturalistic tasks (visual, auditory and sensorimotor; easy and demanding variants pooled). The lines indicate significant connections (task > task-mean), with the different oscillatory frequency bands (6–9, 9–13, 13–20 Hz) plotted in different colors. Note that the 13–20 Hz band was excluded in the auditory task due to a significant difference in signal power between the task and task-mean level. Below the circular connectograms, the connected regions are displayed on the brain surface views. For the color key of the cortical parcellation scheme, see Figure 2. (**B**) Overlap of the connected cortical regions between the task modalities (within-hemisphere analysis): all three tasks overlap (dark red), two tasks overlap (orange), present in one task only (light orange). (**C**) Whole-cortex analysis for the three different task modalities.

power level difference at certain frequency bands were substituted with estimates based on cross-tabulation of factors and proportional values of connections in the conditions (tasks, bands) with no excluded data. Hemispheric lateralization of connectivity was quantified with laterality index LI = (left − right)/(left + right), where positive values indicate left lateralization [Jansen et al., 2006]. In the whole-cortex analysis, interhemispheric connections were categorized and counted as nonhomologous (connections to nonhomologous and nonadjacent regions), near homologous (connections to adjacent regions) and homologous connections (connections to homologous regions).

These connectivity results were studied further on a coarser lobar level where eight lobar areas were collapsed from the 75 parcelled regions. These eight lobar areas were inferior frontal (regions left 69, 72, 73; right 3, 4, 6, 7, 10), superior frontal (regions left 70, 71, 74, 75; right 1, 2, 5, 8, 9), interior parietal (regions left 47–50, 66, 67; right 12, 13, 28–31), superior parietal (regions left 51, 52, 68; right 11, 26, 27), inferior temporal (regions left 44, 54–56, 58, 59;

right 19, 20, 22–24, 33), superior temporal (regions left 57, 60–63; right 15–18, 21), occipital (regions left 39–43; right 34–38), and posteromedial cortex (regions left 45, 46, 53, 64, 65; right 14, 25, 32). At the lobar level, the coherent connections were characterized with graph network measures by calculating degree centrality (unweighted edges; frequency bands pooled) for each lobar area as well as edge degree that counts the interregional significant connections between the lobes [https://sites.google.com/site/bctnet/Home; Sporns et al., 2007]. The lobar nodes with the highest degree centrality were identified as hub regions.

RESULTS

Coherent Connectivity within the Oscillatory 6–20 Hz Range Forms Distinct Patterns for Different Naturalistic Tasks

Coherent oscillatory connections were mapped from the MEG sensor data into the human cortex (see Materials and Methods; [Gross et al., 2001; Kujala et al., 2008]) in the frequency bands of 6–9 Hz (theta/low-alpha), 9–13 Hz (high-alpha) and 13–20 Hz (low-beta). This frequency range (6–20 Hz) featured distinct peaks in the sensor-level coherence spectra, consistently across the studied tasks, indicating oscillatory (narrow-band) signaling that was distinguishable from the spectrally more diffuse high-frequency activity (>30 Hz) (Fig. 1; see Materials and Methods).

The present data-driven, all-to-all interregional mapping (in a parcelled cortex; Fig. 2) showed distinct spatiospectral patterns of coherent connectivity for the different naturalistic tasks, as illustrated in Figure 3 for all three modalities (visual, auditory, sensorimotor). Task-sensitive connectivity was quantified as enhanced coherence with respect to the generic task-mean level [paired $t(9)$-tests, task > task-mean, $P < 0.05$, FDR corrected]. For the majority of the contrasts (task versus task-mean), no parallel change of signal power was observed at the studied spectral bands, but the 13–20 Hz band of the speech comprehension tasks was excluded because of significant power difference [paired $t(9)$-tests, task > task-mean, $P < 0.05$, FDR corrected]. The mean change of coherence varied between 13% and 20% across the tasks. As anatomical connectivity is markedly stronger within than across hemispheres [Hagmann et al., 2008], functional connectivity was first evaluated separately within each hemisphere and then across the whole cortex to trace interhemispheric connections.

In the within-hemisphere analysis (Fig. 3A), the visual modality (picture comparison, left) showed salient right-hemispheric connectivity between the occipital, temporal and parietal cortices. Furthermore, there were connections between the right frontal and parietal cortices. The auditory modality (speech comprehension, middle) showed connectivity joining the left temporal cortex to the frontal and parietal cortices. There were also right-hemispheric cingulo-occipital and frontotemporal connections. The dense connectivity pattern of the sensorimotor modality (object manipulation, right) displayed salient connections between the parietal and frontal cortices.

Of the studied 75 cortical regions, 3 regions contributed to the task-sensitive networks in all three modalities (regions 1, 45, 50; see Fig. 2) and 31 regions contributed to the networks in two modalities (Fig. 3B). Eight regions did not contribute to any of the networks (regions 17, 20, 25, 26, 35, 40, 42, 60). The overlapping regions were found in the ventral and medial frontoparietal, inferior temporo-occipital and posteromedial cortices. Despite the nodal overlap, the connectivity pattern itself was variable across the tasks (Fig. 3A). Taking the nodal region in the left inferior parietal gyrus (region 50) as an example, it was connected to the fusiform gyrus (region 44) at 13–20 Hz in the visual modality, to the superior temporal gyrus (regions 61, 62) at 9–13 Hz in the auditory modality and to the postcentral gyrus, paracentral lobule, posterior cingulate and lingual gyrus (regions 41, 53, 64, 68) at 9–13/13–20 Hz in the sensorimotor modality.

When the whole cortex was simultaneously considered in the analysis (Fig. 3C), the pattern of intrahemispheric connectivity was generally congruent with the within-hemisphere analysis, although not every within-hemisphere connection reached significance in this more widely inclusive analysis (see, e.g., the frontoparietal connectivity in the visual modality or the left perisylvian connectivity in the auditory modality; Fig. 3A). Half of the task-sensitive interhemispheric connections were nonhomologous (51% of all interhemisperic connections). The homologous (7% of all interhemispheric connections) or near homologous (to adjacent regions; 42% of connections) connectivity included, for example, the connection joining the left and right superior parietal gyri (regions 26 and 52) in the sensorimotor task (Fig. 3C).

The Sub-bands of the 6–20 Hz Range Are Emphasized Differently in Different Tasks and Cortical Areas

The task modality (visual, auditory, sensorimotor) and frequency band (6–9, 9–13, 13–20 Hz) were not independent factors as regards the distribution of coherent connections [$\chi^2(4,\ N=163) = 33.4,\ P < 0.001$; see Fig. 3A]. Evaluated with the adjusted standardized residuals ($-1.96 < z < 1.96$), the visual modality showed a higher than expected number of connections in the 6–9 Hz range (z-score 5.1; observed/expected 15/5) and a lower than expected number in the 13–20 Hz range (z-score −3.4; 16/25). Reversely, the sensorimotor task displayed a higher than expected number of connections in the 13–20 Hz band (z-score 3.0; 66/57) and a lower than expected number in the 6–9 Hz band (z-score −5.2; 1/12). The auditory

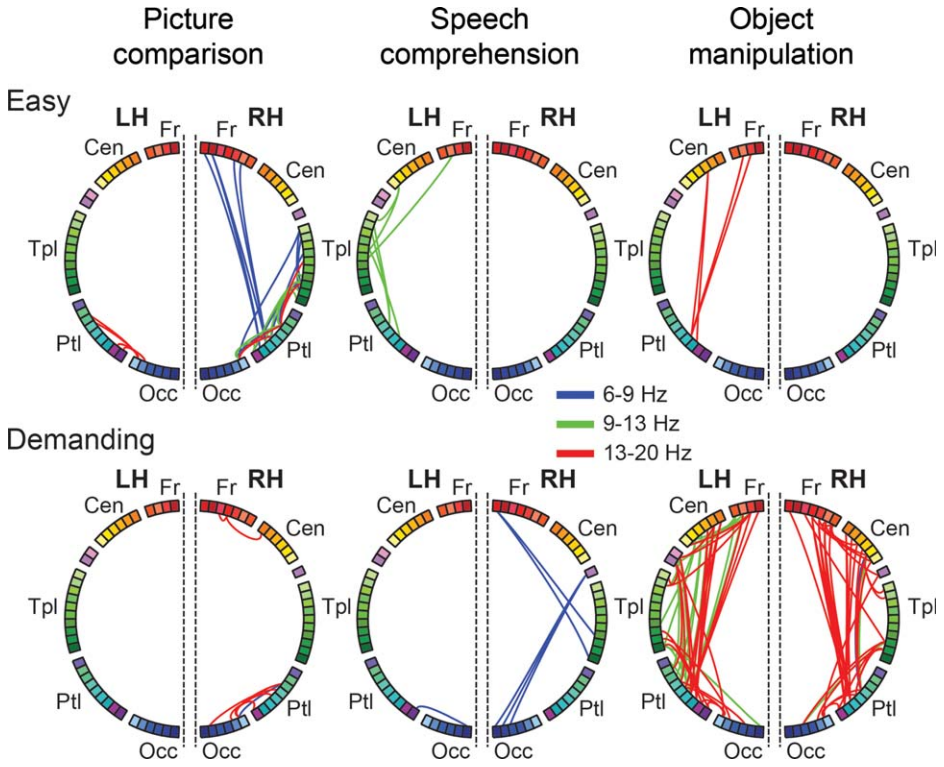

Figure 4.

Effect of task difficulty on the coherent connectivity. Circular connectograms (wihin-hemisphere analysis) for the easy (E) and demanding (D) variants of each task (task > task-mean). For the key of the cortical parcellation scheme, see Figure 2.

modality did not differ from the expected pattern (note that the 13–20 Hz band was excluded and missing values were estimated: *z*-score 0; estimated/expected 20/20).

Across the tasks, the cortical area (frontal, central, cingulate, temporal, parietal, occipital; see Fig. 3A) and frequency band were not independent factors [$\chi^2(10, N = 328) = 26.0$, $P < 0.005$; missing values estimated]. The 6–9 Hz band was utilized less than expected by the central regions (*z*-score −2.3; 1/6). The 9–13 Hz band was utilized more than expected by the temporal cortex (*z*-score 2.4; 19/12) and less than expected by the frontal (*z*-score −2.2; 6/12) and occipital cortices (*z*-score −2.7; 4/11). The 13–20 Hz band was utilized less than expected by the temporal cortex (*z*-score −3.4; 22/33). Spectral patterning in the parietal and cingulate cortices did not deviate from the expected pattern.

The Easy and Demanding Tasks Recruit Functional Networks with Different Emphasis

The task-sensitive connectivity results are illustrated in Figure 4, separately for the easy (E) and demanding (D) variants of the naturalistic tasks (contrasts to the task-mean pattern). Direct pair-wise comparisons of the connections in the easy and demanding tasks did not generally reach significance [paired *t*(9)-tests, E > D or D > E,

TABLE I. Number of significant coherent connections for each task modality and difficulty level in three frequency bands of interest (within-hemisphere analysis).

	Visual		Auditory		Sensorimotor	
Frequency (Hz)	E	D	E	D	E	D
6–9	14	1	0	6	0	1
9–13	9	0	6	0	0	24
13–20	9	7	–	–	4	62

Abbreviations: E: easy; D: demanding; –: excluded due to significant power difference.

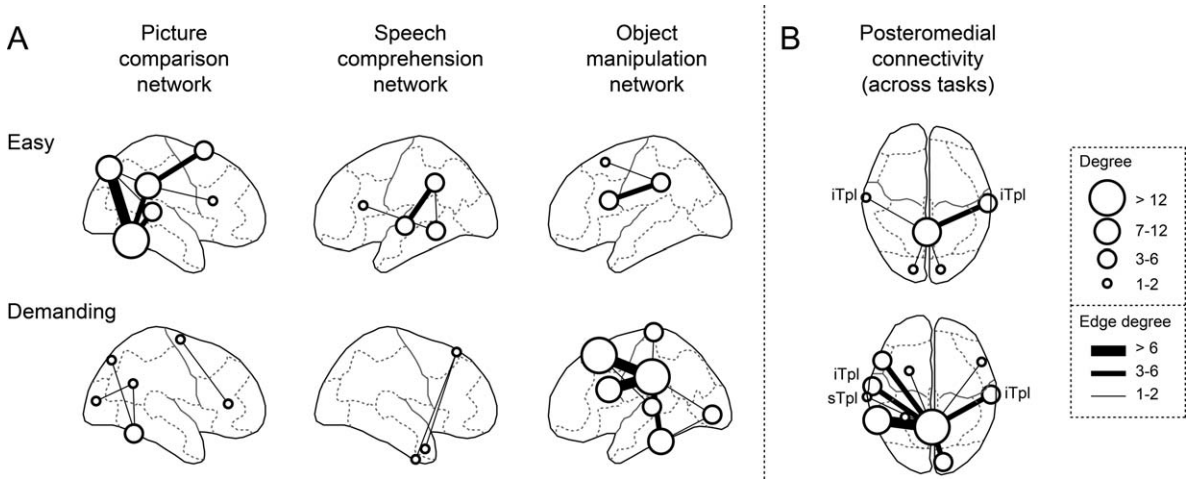

Figure 5.

Graph analysis of task-sensitive connectivity at the lobar level. The parcellated 75 cortical regions (cf. Fig. 2) were combined into 8 lobar level clusters (inferior/superior frontal; inferior/superior parietal; inferior-middle/superior temporal; occipital; posteromedial cortex). The circle size of the cluster nodes represents degree (the number of unweighted intercluster connections from the node, frequencies pooled), and the line width of the connections represents edge degree (the number of connections between the regions of two clusters). (**A**) Coherent networks for each naturalistic task (easy task variant, upper row; more demanding variant, lower row). Node positioning within the lobar cluster area was weighted by the degree of the connected regions. Connections to the posteromedial cortex are not shown. (**B**) Connectivity of the posteromedial cortex, pooled across task modalities. The temporal cortex nodes (iTpl, inferior temporal cortex; sTpl, superior temporal cortex) are located outside of the displayed top view.

$P > 0.05$, FDR corrected; only a single connection showed significantly stronger coherence in the Rubik's cube solution than cube manipulation task]. However, the number of significant coherent connections (task > task-mean; Table I) deviated from an equal pattern across the tasks [pooled across the frequency bands; $\chi^2(5, N = 163) = 177.7$, $P < 0.001$; missing values estimated]. The demanding sensorimotor (Rubik's) task showed the most numerous connections (z-score 11.5; observed/expected 87/27), whereas the demanding visual (z-score −3.7; 8/27), easy auditory (z-score −3.3; 10/27) and easy sensorimotor tasks (z-score −4.4; 4/27) showed less than expected amount of connections (see Table I for each frequency band).

There were core patterns of connectivity for the visual (fusiformal-parietal connectivity) and sensorimotor (frontoparietal connectivity) tasks that were highlighted in both the easy and demanding variants of the tasks. In the speech comprehension task, the significant connections in the easy and demanding conditions emphasized different components of the network: the left perisylvian connectivity at 9–13 Hz did not reach significance in the demanding (non-native) task but, instead, there was connectivity at 6–9 Hz involving markedly the occipital regions. The connectivity pattern observed in the demanding speech condition was salient also in the whole-cortex connectivity analysis (Fig. 3C). In fact, all the significant connections found in the whole-cortex analysis were related to the demanding task in the speech comprehension and object manipulation tasks, whereas the easy condition dominated in the visual task (85% of all connections within the modality).

The number of task-sensitive connections (pooled across frequency bands) showed distinct lateralization for the different tasks (see Fig. 4). The right hemisphere predominated in the visual task (laterality index LI = −0.7 easy, LI = −1.0 demanding). In the auditory task, the pattern changed from left lateralized (LI = +1.0) in the easy condition to right lateralized in the demanding condition (LI = −0.7). In the sensorimotor task, the left-lateralized pattern (LI = +1.0) in the easy condition became bilateral (LI = +0.1) in the demanding condition. In the more bilateral maps, the parieto-occipital connections in the visual task and the frontoparietal connections in the sensorimotor task were mirrored in the nondominant hemisphere.

Lobar level graph plots (Fig. 5A; see Materials and Methods) illustrate the coherent networks for the easy and demanding tasks within the hemisphere that is dominant for the task. In picture comparison, there was a main hub in the right inferior temporal cortex. In the easier variant, the highest edge degree was found between this inferotemporal hub region and the posterior superior parietal cortex. The demanding variant displayed a generally lower degree of connectivity. In speech comprehension, the main hub in the easy condition was located in the left inferior parietal cortex that had a high-degree linkage to the left superior temporal cortex. The demanding speech comprehension highlighted right-hemisphere connection between

anterior temporal and superior frontal cortices, along with the midline cingulo-occipital connectivity (Figs. 3C, 4). In object manipulation, the main hub was located in the left inferior parietal cortex that connected to the inferior and superior frontal cortices. The edge degree for the frontoparietal connectivity was notably high in the demanding task variant, and connectivity emerged between the occipital, temporal, and parietal cortices. Across the tasks (Fig. 5B), the posteromedial cortex showed higher degree and edge degree for the demanding than easier variants, with coherent connections formed particularly with the bilateral temporal and the left inferior parietal cortices.

DISCUSSION

The key objective of the present human MEG study was to gain a cortex-wide view on task-sensitivity of coherent oscillatory connectivity in association with naturalistic performance. As hypothesized, the data-driven mapping of long-range coherence revealed task-sensitive reconfiguration of global connectivity patterns for a set of naturalistic tasks. The elevated 6–20 Hz long-range coherence was differentially routed for each task, in comparison with the generic task-mean pattern. The connectivity patterns were well formed as each type of naturalistic behavior was associated with topologically task-relevant connectivity patterns. The different corticocortical task networks utilized the studied oscillatory bands (6–9, 9–13, 13–20 Hz) to a varying degree. The networks engaged both nodal regions that were distinct for each task modality and others that were more overlapping between modalities (including frontoparietal cortex). Overall, the present study uncovered flexible spatiospectral patterning of coherent connectivity that forms well-defined functional network structures to support different naturalistic behaviors.

Task-Sensitive 6–20 Hz Coherence

The task-sensitive coherent connectivity was mapped within the 6–20 Hz oscillatory range which has been eminently linked with long-range interregional coupling and neurocommunication [Kopell et al., 2000; von Stein and Sarnthein, 2000]. Spectrally narrow-band oscillatory activity is prominent at the <30 Hz neural frequencies, whereas the higher frequencies (>30 Hz; low/high-gamma band) encompass both oscillatory and arrythmic broadband signaling [e.g., Bressler et al., 1993; Buzsáki and Draguhn, 2004; Crone et al., 2006; Hari and Salmelin, 1997]. The lower-frequency oscillations may coordinate and interact with the high-frequency activity [Buschman et al., 2012; Lisman and Jensen, 2013] and, in some instances, emerge as concatenation of higher frequency signals [Kopell et al., 2011]. The spectral content, or fingerprint, of connectivity may index specific computation performed in the cortical microcircuitry [Bastos et al., 2012; Siegel et al., 2012]. The oscillatory frequencies studied here have been associated with maintained, semistable states and feedback-type corticocortical interactions [Cannon et al., 2014; Siegel et al., 2012; van Kerkoerle et al., 2014; von Stein et al., 2000] rather than more transient, feedforward-type responses [associated recently with frequencies >30 Hz and <6 Hz; Bastos et al., 2015]. Oscillatory interaction at 6–20 Hz has been proposed to play a role in various neurocognitive processes, such as memory retention, multimodal processing, rule-switching and decisional performance [Buschman et al., 2012; Cannon et al., 2014; Fell and Axmacher, 2011; Kopell et al., 2011; Pesaran et al., 2008], all important for naturalistic behavior.

The subbands of the 6–20 Hz range were differently emphasized in the tasks: whereas the picture comparison task relied heavily on the lowest (6–9 Hz) band, the object manipulation task utilized particularly the highest band (13–20 Hz), instead. The pronounced theta/low-alpha coherence (6–9 Hz) in the naturalistic picture comparison task agrees with earlier primate and human findings on visuo-attentional and working memory performance [Landau and Fries, 2012; Liebe et al., 2012; Watrous et al., 2013]. Interregional theta coupling has been linked with memory maintenance of visual material [Fell and Axmacher, 2011; Liebe et al., 2012] as well as with attentional reorienting to unexpected stimuli in the frontoparietal network [Daitch et al., 2013]. The prominent low-beta coherence (13–20 Hz) for the sensorimotor task has been found also in the monkey frontoparietal cortex [Pesaran et al., 2008]. The wider beta band (15–30 Hz) has been associated with motor function [Brovelli et al., 2004; Salenius and Hari, 2003]. The frontoparietal low-beta band interaction can be related to cognitive aspects of active motor performance [Cannon et al., 2014; Pesaran et al., 2008] rather than pure movement patterning [cf. Gross et al., 2002].

The spectral subbands also differed in their topological emphasis. The temporal regions relied less on the highest (13–20 Hz) band and the frontocentral regions less on the lowest bands (6–9 Hz/9–13 Hz). This finding parallels the task-sensitive pattern where the picture comparison task, involving the temporal visual regions, relied relatively more on the theta/low-alpha band compared to the low-beta band. The object manipulation task, involving the frontocentral motor regions, showed a reversed pattern. This indicates that cortical topology and task-related spectral patterning are intertwined. Conversely, when network nodes were found in regions that are known to generate prominent spontaneous rhythms [at rest; Hari and Salmelin, 1997], such nodes did not seem to consistently utilize the spontaneous oscillatory bands for their coherent connectivity: the occipital regions did not primarily link to other areas at the high-alpha band of the posterior spontaneous rhythm [Hari and Salmelin, 1997], and the temporal regions relied on the high-alpha band [cf. Bonte et al., 2009] rather than on the theta/low-alpha band activity [spontaneous "tau" rhythm; Lehtelä et al., 1997] to connect with other areas.

Reconfiguration of Coherent Connectivity for Naturalistic Tasks

Previous imaging studies on electrophysiological connectivity have largely focused on spontaneous rest activity [e.g., Brookes et al., 2011; Hipp et al., 2012] or on fairly restricted, single-domain experimental paradigms in visual [e.g., Gross et al., 2004; Palva et al., 2010; Siegel et al., 2008], language [e.g., Alho et al. 2014; Kujala et al., 2007, 2012; Liljeström et al., 2015] and motor domains [e.g., Gross et al., 2002; Jerbi et al., 2007; Pollok et al., 2005]. A naturalistic approach has since emerged to complement these results, as exemplified by research on natural vision [Betti et al., 2013; Watrous et al., 2013].

In the present study, the focus was on active, continuous performance of low-constrained tasks, with meaningful stimuli. In primates, long-range coherence has been enhanced by low-constrained tasks that require active decisional performance [Pesaran et al., 2008]. In ecological settings, neurocognition adapts to serve active behavior [Kingstone et al., 2008]. For understanding the brain–behavior relationship, naturalistic experimental approaches can importantly complement the more constrained designs that are often, unavoidably, rather artificial [see Felsen and Dan, 2005; Hasson et al., 2010; Ingram and Wolpert, 2011]. The naturalistic approach is likely to highlight behaviorally significant patterns of functional connectivity.

The present data-driven analysis of enhanced 6–20 Hz coherence in naturalistic tasks uncovered task-relevant hubs and coherent connections that are in good harmony with previous activation-, stimulation-, and lesion-based descriptions of human cortical organization. In the picture comparison task, coherent connections emerged between the temporo-occipital hub region in the ventral (object/color-related) visual stream and the higher-order nodes of the dorsal (spatial/motor-related) stream [Goodale and Milner, 1992; Zeki and Marini, 1998]. The right-hemispheric frontoparietal connectivity agrees with the attention-related cortical networks [Corbetta and Shulman, 2002, 2011]. The easy speech comprehension task highlighted coherent connectivity of central cortical regions with the left perisylvian cortex [Hickok and Poeppel, 2007; Turken and Dronkers, 2011], in line with the suggested ventral temporofrontal (speech recognition/meaning-related) and dorsal temporoparietal-frontal (articulation-related) cortical streams for speech perception [Hickok and Poeppel, 2007; Rauschecker and Scott, 2009]. In the object manipulation task, the main hub was observed in the left inferior parietal cortex that connected with the frontal cortex. This pattern is in good agreement with activation and stimulation studies on intentionally guided manual behavior [Binkofski et al., 1999; Desmurget et al., 2009; Haaland and Harrington, 1996; Rizzolatti and Sinigaglia, 2010].

The demanding variants of the tasks, as contrasted to the task-mean pattern, emphasized partly different components of the network, possibly reflecting differential predominance of distinct neurocognitive states in the demanding versus easy task. In the demanding picture comparison task, the relative emphasis was on the frontofrontal low-beta coherence [cf. Womelsdorf et al., 2014] rather than the frontoparietal theta/low-alpha connectivity [cf. Daitch et al., 2013]. This may highlight the difference in strategy between the pop-up-type, stimulus-driven search in the easy comparison task and the more top-down-driven processing in the demanding task [cf. Buschman and Miller, 2007]. In the non-native speech comprehension, there was prominent connectivity involving the occipital visual regions (particularly the whole-cortex analysis) that may relate to visual imagery [Kosslyn et al., 1999] elicited by the movie soundtrack clips, without direct visual stimulation. The anterior temporal to frontal connectivity may reflect higher-order semantic processing [Visser et al., 2010]. The demanding Rubik's task that required both object manipulation and visuospatial reasoning strongly engaged the frontoparietal connections [Binkofski et al., 1999; Corbetta and Shulman, 2002], as well as the visual system [Goodale and Milner, 1992]. The most numerous connectivity (at 6–20 Hz) observed in the Rubik's task may be partly associated with the task requirement of active reasoning rather than automatic, rule-based performance [cf. Buschman et al., 2012].

The distinct task-sensitive patterns were complemented by a subset of network nodes that participated in the coherent networks regardless of the naturalistic task modality, thus reflecting regional one-to-many organization [cf. Mesulam, 2008]. There was prominent overlap of nodal regions in the frontoparietal cortex that is thought to form a multitask core structure in distributed neurocognitive architecture [Barbey et al., 2012; Duncan, 2010; Fox et al., 2005]. A major region of this overlap emerged in the (left) inferior parietal cortex, an associative region identified as an important hub of the human lateral cortex [Sepulcre et al., 2012]. Furthermore, task-independent nodes were found in the medial frontal and cingulate cortices, regions previously linked to a rich-club-type backbone of the cortical network [van den Heuvel et al., 2012]. The posteromedial cortex, including the cingulate cortex, constitutes the major cortical hub of the resting-state activity [Greicius et al., 2003; Hagmann et al., 2008; Raichle, 2010]. The significant role for the posteromedial cortex in effortful task performance in the present data supports the view that this central hub is not merely involved in purely intrinsic, task-negative function [Fox et al., 2005; Greicius et al., 2003; Raichle, 2010].

Cortex-Wide Mapping of Task-Sensitive Coherence

The all-to-all MEG mapping of interregional coherence in the human cortex extends the intracortical primate studies on singular task-sensitive coherent connections. Noninvasive electromagnetic brain imaging facilitates reliable

estimation of long-range corticocortical connectivity in the intact human brain [when method-inherent confounds and artifactual sources of signals (see Materials and Methods) are properly taken into account; Hipp and Siegel, 2013; Kujala et al., 2008, 2012; Schoffelen and Gross, 2009]; estimation of short-range connectivity is problematic because of the field spread of the electromagnetic signal [Schoffelen and Gross, 2009]. MEG reflects population-level dendritic activity in the cortical pyramidal cells [Hämäläinen et al., 1993; Okada et al., 1997], a measure that has a cellular-level counterpart in the local field potential (LFP) recordings [Buzsáki et al., 2012]. LFP signals in the primate cortex show interregional coherence between task-sensitive subpopulations of neurons [Buschman and Miller, 2007; Salazar et al., 2012] and are coupled with the spiking activity of the cells in the functionally connected cortical regions [Gregoriou et al., 2009; Pesaran et al., 2008]. In descriptive terms, neural coherence is a dynamic property of interregional signaling but, theoretically, it can also be regarded as a key mechanism for neuronal information processing.

The present results can be taken to support the hypothesis that oscillatory coherence plays a key role in the cortical implementation of neurocognition [Bressler and Kelso, 2001; Engel et al., 2013; Fries, 2005; Siegel et al., 2012]. Mechanistically, electrophysiological oscillations in dendrites can provide periodically opening temporal windows for effective neuronal communication [Fries, 2005; Izhikevich, 2001], and long-range coherence of these oscillatory signals can facilitate temporal coordination and interregional routing in the network signaling [Akam and Kullmann, 2010; Bosman et al., 2012; Engel et al., 2013; Siegel et al., 2012; Varela et al., 2001]. The exact functional interpretation of coherence depends on anatomical scaffolding, as tightly and bidirectionally connected regions, such as the frontal and parietal cortex, can engage in reciprocal hand-shake-type oscillatory interaction [Pesaran et al., 2008]; however, coherence can also reflect indirect, cortically, or subcortically mediated connections and thus more widespread synchrony in the brain network [Haider and McCormick, 2009; Saalmann et al., 2012; Siegel et al., 2012; Varela et al., 2001]. Here, the results do not dissociate between such different network configurations but, instead, they offer an overview of elevated coherent episodes occurring in the cortical networks in association with various naturalistic tasks.

The coherence mapping uncovered real-time task-sensitive oscillatory components of functional connectivity, instead of focusing on connectivity patterns that persist across task and rest periods alike [Power et al., 2011; Smith et al., 2009; Yeo et al., 2011]. The current approach agrees with electrophysiological studies that track oscillatory interaction (coherence, phase stability etc.) at the millisecond scale [Bressler and Kelso, 2001; Palva and Palva, 2012; Siegel et al., 2012] and differ from the slower-scale characterizations of band-passed power envelope correlation [Brookes et al., 2011; Hipp et al., 2012] and hemodynamic comodulation [Cole et al., 2013; Power et al., 2011; Yeo et al., 2011]. The millisecond-scale connectivity has been linked to on-going, task-related neuronal processing, whereas the slower-scale modulations presumably represent an intrinsic coupling mode related to the more general state or history of the network [Engel et al., 2013; Siegel et al., 2012]. A correspondence between such faster- and slower-scale characterizations is not straightforward. For example, electrophysiological power envelopes may be correlated at the low-beta band [e.g. Hipp et al., 2012] but such correlations are suppressed by task [Betti et al., 2013], unlike the millisecond-scale coherence that shows salient task-dependent enhancement. Conversely, the electrophysiological <20 Hz activity may correlate particularly well with the hemodynamic measures of functional connectivity [Wang et al., 2012].

Neurocognitive networks are widely considered an important concept in understanding brain function [Friston, 2008; Mesulam, 2008]. In the future, it will be important to deepen the understanding of the relationships between the intracranial and noninvasive electrophysiological and hemodynamic measures of functional connectivity, and of the way they capture network function in different behaviorally relevant tasks [see Betti et al., 2013; Park and Friston, 2013]. The present distinct connectivity patterns in varied naturalistic tasks provide an essential data-driven reference set for that important endeavor.

CONCLUSIONS

The present noninvasive mapping of task-sensitive long-range coherence shows that the human cortex self-organizes into distinct spatiospectral patterns of interregional coherence to support naturalistic behavior. These findings provide empirical evidence that coherent oscillatory interaction at the narrow-band (<30 Hz) neuronal frequencies plays a significant role in the cortical implementation of neurocognition.

ACKNOWLEDGMENTS

The authors thank Hannu Laaksonen and Mia Liljeström for comments on the manuscript. The authors declare no competing financial interests.

REFERENCES

Akam T, Kullmann DM (2010): Oscillations and filtering networks support flexible routing of information. Neuron 67:308–320.

Alho J, Lin FH, Sato M, Tiitinen H, Sams M, Jääskeläinen IP (2014): Enhanced neural synchrony between left auditory and premotor cortex is associated with successful phonetic categorization. Front Psychol 5:394.

Barbey AK, Colom R, Solomon J, Krueger F, Forbes C, Grafman J (2012): An integrative architecture for general intelligence and executive function revealed by lesion mapping. Brain 135: 1154–1164.

Bastos AM, Usrey WM, Adams RA, Mangun GR, Fries P, Friston KJ (2012): Canonical microcircuits for predictive coding. Neuron 76:695–711.

Bastos AM, Vezoli J, Bosman CA, Schoffelen JM, Oostenveld R, Dowdall JR, de Weerd P, Kennedy H, Fries P (2015): Visual areas exert feedforward and feedback influences through distinct frequency channels. Neuron 85:390–401.

Betti V, Della Penna S, de Pasquale F, Mantini D, Marzetti L, Romani GL, Corbetta M (2013): Natural scenes viewing alters the dynamics of functional connectivity in the human brain. Neuron 79:782–797.

Binkofski F, Buccino G, Posse S, Seitz RJ, Rizzolatti G, Freund H (1999): A fronto-parietal circuit for object manipulation in man: Evidence from an fMRI-study. Eur J Neurosci 11:3276–3286.

Bonte M, Valente G, Formisano E (2009): Dynamic and task-dependent encoding of speech and voice by phase reorganization of cortical oscillations. J Neurosci 29:1699–1706.

Bosman CA, Schoffelen JM, Brunet N, Oostenveld R, Bastos AM, Womelsdorf T, Rubehn B, Stieglitz T, De Weerd P, Fries P(2012): Attentional stimulus selection through selective synchronization between monkey visual areas. Neuron 75:875–888.

Bressler SL, Kelso JA (2001): Cortical coordination dynamics and cognition. Trends Cogn Sci 5:26–36.

Bressler SL, Coppola R, Nakamura R (1993): Episodic multiregional cortical coherence at multiple frequencies during visual task performance. Nature 366:153–156.

Brookes MJ, Woolrich M, Luckhoo H, Price D, Hale JR, Stephenson MC, Barnes GR, Smith SM, Morris PG (2011): Investigating the electrophysiological basis of resting state networks using magnetoencephalography. Proc Natl Acad Sci USA 108:16783–16788.

Brovelli A, Ding M, Ledberg A, Chen Y, Nakamura R, Bressler SL (2004): Beta oscillations in a large-scale sensorimotor cortical network: Directional influences revealed by Granger causality. Proc Natl Acad Sci USA 101:9849–9854.

Buschman TJ, Miller EK (2007): Top-down versus bottom-up control of attention in the prefrontal and posterior parietal cortices. Science 315:1860–1862.

Buschman TJ, Denovellis EL, Diogo C, Bullock D, Miller EK (2012): Synchronous oscillatory neural ensembles for rules in the prefrontal cortex. Neuron 76:838–846.

Buzsáki G, Draguhn A (2004): Neuronal oscillations in cortical networks. Science 304:1926–1929.

Buzsáki G, Anastassiou CA, Koch C (2012): The origin of extracellular fields and currents - EEG, ECoG, LFP and spikes. Nat Rev Neurosci 13:407–420.

Cannon J, McCarthy MM, Lee S, Lee J, Börgers C, Whittington MA, Kopell N (2014): Neurosystems: Brain rhythms and cognitive processing. Eur J Neurosci 39:705–719.

Cole MW, Reynolds JR, Power JD, Repovs G, Anticevic A, Braver TS (2013): Multi-task connectivity reveals flexible hubs for adaptive task control. Nat Neurosci 16:1348–1355.

Corbetta M, Shulman GL (2002): Control of goal-directed and stimulus-driven attention in the brain. Nat Rev Neurosci 3:201–215.

Corbetta M, Shulman GL (2011): Spatial neglect and attention networks. Annu Rev Neurosci 34:569–599.

Crone NE, Sinai A, Korzeniewska A (2006): High-frequency gamma oscillations and human brain mapping with electrocorticography. Prog Brain Res 159:275–295.

Daitch AL, Sharma M, Roland JL, Astafiev SV, Bundy DT, Gaona CM, Snyder AZ, Shulman GL, Leuthardt EC, Corbetta M (2013): Frequency-specific mechanism links human brain networks for spatial attention. Proc Natl Acad Sci USA 110: 19585–19590.

Desikan, RS, Ségonne, F, Fischl, B, Quinn, BT, Dickerson, BC, Blacker, D, Buckner, RL, Dale, AM, Maguire, RP, Hyman, BT, Albert MS, Killiany RJ (2006): An automated labeling system for subdividing the human cerebral cortex on MRI scans into gyral based regions of interest. Neuroimage 31:968–980.

Desmurget M, Reilly KT, Richard N, Szathmari A, Mottolese C, Sirigu, A(2009): Movement intention after parietal cortex stimulation in humans. Science 24:811–813.

Duncan J (2010): The multiple-demand (MD) system of the primate brain: Mental programs for intelligent behaviour. Trends Cogn Sci 14:172–179.

Engel AK, Gerloff C, Hilgetag CC, Nolte G (2013): Intrinsic coupling modes: Multiscale interactions in ongoing brain activity. Neuron 80:867–886.

Fell J, Axmacher N (2011): The role of phase synchronization in memory processes. Nat Rev Neurosci 12:105–118.

Felsen G, Dan, Y (2005): A natural approach to studying vision. Nat Neurosci 8:1643–1646.

Fox MD, Snyder AZ, Vincent JL, Corbetta M, Van Essen DC, Raichle, ME (2005): The human brain is intrinsically organized into dynamic, anticorrelated functional networks. Proc Natl Acad Sci USA 102:9673–9678.

Fries P (2005): A mechanism for cognitive dynamics: Neuronal communication through neuronal coherence. Trends Cogn Sci 9:474–480.

Friston K (2008): Hierarchical models in the brain. PLoS Comput Biol 4:e1000211.

Goodale MA, Milner AD (1992): Separate visual pathways for perception and action. Trends Neurosci 15:20–25.

Gregoriou GG, Gotts SJ, Zhou H, Desimone R (2009): High-frequency, long-range coupling between prefrontal and visual cortex during attention. Science 324:1207–1210.

Greicius MD, Krasnow B, Reiss AL, Menon V (2003): Functional connectivity in the resting brain: A network analysis of the default mode hypothesis. Proc Natl Acad Sci USA 100:253–258.

Gross J, Kujala J, Hämäläinen M, Timmermann L, Schnitzler A, Salmelin R (2001): Dynamic imaging of coherent sources: Studying neural interactions in the human brain. Proc Natl Acad Sci USA 98:694–699.

Gross J, Schmitz F, Schnitzler I, Kessler K, Shapiro K, Hommel B, Schnitzler A (2004): Modulation of long-range neural synchrony reflects temporal limitations of visual attention in humans. Proc Natl Acad Sci USA 101:13050–13055.

Gross J, Timmermann L, Kujala J, Dirks M, Schmitz F, Salmelin R, Schnitzler A (2002): The neural basis of intermittent motor control in humans. Proc Natl Acad Sci USA 99:2299–2302.

Haaland KY, Harrington DL (1996): Hemispheric asymmetry of movement. Curr Opin Neurobiol 6:796–800.

Hagmann P, Cammoun L, Gigandet X, Meuli R, Honey CJ, Wedeen VJ, Sporns O (2008): Mapping the structural core of human cerebral cortex. PLoS Biol 6:e159.

Haider B, McCormick DA (2009): Rapid neocortical dynamics: Cellular and network mechanisms. Neuron 62:171–189.

Hämäläinen MS, Hari R, Ilmoniemi RJ, Knuutila J, Lounasmaa O (1993): Magnetoencephalography - theory, instrumentation, and applications to noninvasive studies of the working human brain. Rev Mod Phys 65:413–507.

Hari R, Salmelin R (1997): Human cortical oscillations: A neuromagnetic view through the skull. Trends Neurosci 20:44–49.

Hasson U, Malach R, Heeger DJ (2010): Reliability of cortical activity during natural stimulation. Trends Cogn Sci 14:40–48.

Hickok G, Poeppel D (2007): The cortical organization of speech processing. Nat Rev Neurosci 8:393–402.

Hipp JF, Hawellek DJ, Corbetta M, Siegel M, Engel AK (2012): Large-scale cortical correlation structure of spontaneous oscillatory activity. Nat Neurosci 15:884–890.

Hipp JF, Siegel M (2013): Dissociating neuronal gamma-band activity from cranial and ocular muscle activity in EEG. Front Hum Neurosci 7:338.

Holten D (2006): Hierarchical edge bundles: Visualization of adjacency relations in hierarchical data. IEEE Trans Vis Comput Graphics 12:741–748.

Ingram JN, Wolpert DM (2011): Naturalistic approaches to sensorimotor control. Prog Brain Res 191:3–29.

Izhikevich EM (2001): Resonate-and-fire neurons. Neural Netw 14: 883–894.

Jansen A, Menke R, Sommer J, Förster AF, Bruchmann S, Hempleman J, Weber B, Knecht S (2006): The assessment of hemispheric lateralization in functional MRI -robustness and reproducibility. Neuroimage 33:204–217.

Jerbi K, Lachaux JP, N'Diaye K, Pantazis D, Leahy RM, Garnero L, Baillet S (2007): Coherent neural representation of hand speed in humans revealed by MEG imaging. Proc Natl Acad Sci USA 104:7676–7681.

Kingstone A, Smilek D, Eastwood JD (2008): Cognitive Ethology: A new approach for studying human cognition. Br J Psychol 99:317–340.

Kopell N, Whittington MA, Kramer MA (2011): Neuronal assembly dynamics in the beta1 frequency range permits short-term memory. Proc Natl Acad Sci USA 108:3779–3784.

Kopell N, Ermentrout GB, Whittington MA, Traub RD (2000): Gamma rhythms and beta rhythms have different synchronization properties. Proc Natl Acad Sci USA 97:1867–1872.

Kosslyn SM, Pascual-Leone A, Felician O, Camposano S, Keenan JP, Thompson WL, Ganis G, Sukel KE, Alpert NM (1999): The role of area 17 in visual imagery: Convergent evidence from PET and rTMS. Science 284:167–170.

Kujala J, Gross J, Salmelin, R(2008): Localization of correlated network activity at the cortical level with MEG. Neuroimage 39: 1706–1720.

Kujala J, Pammer K, Cornelissen P, Roebroeck A, Formisano E, Salmelin R (2007): Phase coupling in a cerebro-cerebellar network at Aug13 Hz during reading. Cereb Cortex 17:1476–1485.

Kujala J, Vartiainen J, Laaksonen H, Salmelin R (2012): Neural interactions at the core of phonological and semantic priming of written words. Cereb Cortex 22:2305–2312.

Landau AN, Fries P (2012): Attention samples stimuli rhythmically. Curr Biol 22:1000–1004.

Lehtelä L, Salmelin R, Hari R (1997): Evidence for reactive magnetic 10-Hz rhythm in the human auditory cortex. Neurosci Lett 222:111–114.

Liebe S, Hoerzer GM, Logothetis NK, Rainer G (2012): Theta coupling between V4 and prefrontal cortex predicts visual short-term memory performance. Nat Neurosci 15:456–462.

Liljeström M, Kujala J, Jensen O, Salmelin R (2005): Neuromagnetic localization of rhythmic activity in the human brain: A comparison of three methods. Neuroimage 25:734–745.

Liljeström M, Kujala J, Stevenson C, Salmelin R (2015): Dynamic reconfiguration of the language network preceding onset of speech in picture naming Hum Brain Mapp 36:1202–1216.

Lisman JE, Jensen O (2013): The Theta-Gamma neural code. Neuron 77:1002–1016.

Mesulam M (2008): Representation, inference, and transcendent encoding in neurocognitive networks of the human brain. Ann Neurol 64:367–378.

Morcom AM, Fletcher PC (2007): Does the brain have a baseline? Why we should be resisting a rest. Neuroimage 37: 1073–1082.

Okada YC, Wu J, Kyuhou S (1997): Genesis of MEG signals in a mammalian CNS structure. Electroencephalogr Clin Neurophysiol 103:474–485.

Palva S, Palva JM (2012): Discovering oscillatory interaction networks with M/EEG: Challenges and breakthroughs. Trends Cogn Sci 16:219–230.

Palva JM, Monto S, Kulashekhar S, Palva S (2010): Neuronal synchrony reveals working memory networks and predicts individual memory capacity. Proc Natl Acad Sci USA 107:7580–7585.

Park HJ, Friston K (2013): Structural and functional brain networks: From connections to cognition. Science 342:1238411.

Pesaran B, Nelson MJ, Andersen RA (2008): Free choice activates a decision circuit between frontal and parietal cortex. Nature 453:406–409.

Pollok B, Südmeyer M, Gross J, Schnitzler A (2005): The oscillatory network of simple repetitive bimanual movements. Brain Res Cogn Brain Res 25:300–311.

Power JD, Cohen AL, Nelson SM, Wig GS, Barnes KA, Church JA, Vogel AC, Laumann TO, Miezin FM, Schlaggar BL, Petersen SE (2011): Functional network organization of the human brain. Neuron 72:665–678.

Raichle ME (2010): Two views of brain function. Trends Cogn Sci 14:180–190.

Rauschecker JP, Scott SK (2009): Maps and streams in the auditory cortex: Nonhuman primates illuminate human speech processing. Nat Neurosci 12:718–724.

Rizzolatti G, Sinigaglia C (2010): The functional role of the parieto-frontal mirror circuit: Interpretations and misinterpretations. Nat Rev Neurosci 11:264–274.

Saalmann YB, Pinsk MA, Wang L, Li X, Kastner S (2012): The pulvinar regulates information transmission between cortical areas based on attention demands. Science 337:753–756.

Salazar RF, Dotson NM, Bressler SL, Gray CM (2012): Content-specific fronto-parietal synchronization during visual working memory. Science 338:1097–1100.

Salenius S, Hari R (2003): Synchronous cortical oscillatory activity during motor action. Curr Opin Neurobiol 13:678–684.

Schoffelen JM, Gross J (2009): Source connectivity analysis with MEG and EEG. Hum Brain Mapp 30:1857–1865.

Sehatpour P, Molholm S, Schwartz TH, Mahoney JR, Mehta AD, Javitt DC, Stanton PK, Foxe JJ (2008): A human intracranial study of long-range oscillatory coherence across a frontal-occipital-hippocampal brain network during visual object processing. Proc Natl Acad Sci USA 105:4399–4404.

Sepulcre J, Sabuncu MR, Yeo TB, Liu H, Johnson KA (2012): Stepwise connectivity of the modal cortex reveals the multimodal organization of the human brain. J Neurosci 32:10649–10661.

Siegel M, Donner TH, Engel AK (2012): Spectral fingerprints of large-scale neuronal interactions. Nat Rev Neurosci 13:121–134.

Siegel M, Donner TH, Oostenveld R, Fries P, Engel AK (2008): Neuronal synchronization along the dorsal visual pathway reflects the focus of spatial attention. Neuron 60:709–719.

Smith SM, Fox PT, Miller KL, Glahn DC, Fox PM, Mackay CE, Filippini N, Watkins KE, Toro R, Laird AR, Beckmann CF (2009): Correspondence of the brain's functional architecture during activation and rest. Proc Natl Acad Sci USA 106:13040–13045.

Sporns O, Honey CJ, Kötter R (2007): Identification and classification of hubs in brain networks. PLoS One 2:e1049.

Swann NC, Cai W, Conner CR, Pieters TA, Claffey MP, George JS, Aron AR, Tandon N (2012): Roles for the pre-supplementary motor area and the right inferior frontal gyrus in stopping action: Electrophysiological responses and functional and structural connectivity. Neuroimage 59:2860–2870.

Taulu S, Simola J (2006): Spatiotemporal signal space separation method for rejecting nearby interference in MEG measurements. Phys Med Biol 51:1759–1768.

Taulu S, Hari R (2009): Removal of magnetoencephalographic artifacts with temporal signal-space separation: Demonstration with single-trial auditory-evoked responses. Hum Brain Mapp 30:1524–1534.

Turken AU, Dronkers NF (2011): The neural architecture of the language comprehension network: Converging evidence from lesion and connectivity analyses. Front Syst Neurosci 5:1.

van den Heuvel MP, Kahn RS, Goñi J, Sporns O (2012): High-cost, high-capacity backbone for global brain communication. Proc Natl Acad Sci USA 109:11372–11377.

van Kerkoerle T, Self MW, Dagnino B, Gariel-Mathis MA, Poort J, van der Togt C, Roelfsema PR (2014): Alpha and gamma oscillations characterize feedback and feedforward processing in monkey visual cortex. Proc Natl Acad Sci USA 111:14332–14341.

Varela F, Lachaux JP, Rodriguez E, Martinerie J (2001): The brainweb: Phase synchronization and large-scale integration. Nat Rev Neurosci 2:229–239.

Visser M, Jefferies E, Lambon Ralph MA (2010): Semantic processing in the anterior temporal lobes: A meta-analysis of the functional neuroimaging literature. J Cogn Neurosci 22:1083–1094.

von Stein A, Chiang C, König P (2000): Top-down processing mediated by interareal synchronization. Proc Natl Acad Sci USA 97:14748–14753.

von Stein A, Sarnthein J (2000): Different frequencies for different scales of cortical integration: From local gamma to long range alpha/theta synchronization. Int J Psychophysiol 38:301–313.

Wang L, Saalmann YB, Pinsk MA, Arcaro MJ, Kastner S (2012): Electrophysiological low-frequency coherence and cross-frequency coupling contribute to BOLD connectivity. Neuron 76:1010–1020.

Watrous AJ, Tandon N, Conner CR, Pieters T, Ekstrom AD (2013): Frequency-specific network connectivity increases underlie accurate spatiotemporal memory retrieval. Nat Neurosci 16: 349–356.

Woestenburg JC, Verbaten MN, Slangen JL (1983): The removal of the eye-movement artifact from the EEG by regression analysis in the frequency domain. Biol Psychol 16:127–147.

Womelsdorf T, Ardid S, Everling S, Valiante TA (2014): Burst firing synchronizes prefrontal and anterior cingulate cortex during attentional control. Curr Biol 24:2613–2621.

Yeo BT, Krienen FM, Sepulcre J, Sabuncu MR, Lashkari D, Hollinshead M, Roffman JL, Smoller JW, Zöllei L, Polimeni JR, Fischl B, Liu H, Buckner RL (2011): The organization of the human cerebral cortex estimated by intrinsic functional connectivity. J Neurophysiol 106:1125–1165.

Zeki S, Marini L (1998): Three cortical stages of colour processing in the human brain. Brain 121:1669–1685.